

Ultralow-threshold $\text{Yb}^{3+}:\text{SiO}_2$ glass laser fabricated by the solgel process

Eric P. Ostby,^{1,*} Lan Yang,^{1,2} and Kerry J. Vahala¹

¹Department of Applied Physics, California Institute of Technology, Pasadena, California 91125, USA

²Present address, Department of Electrical and Systems Engineering, Washington University, St. Louis, Missouri 63130, USA

*Corresponding author: ostby@caltech.edu

Received July 5, 2007; accepted July 25, 2007;
posted August 3, 2007 (Doc. ID 84873); published September 4, 2007

A Yb-doped silica microcavity laser on a silicon chip is fabricated from a solgel thin film. The high- Q microtoroid cavity, which has a finesse of 10,000, is evanescently coupled to an optical fiber taper. We report a threshold of 1.8 μW absorbed power that is, to the best of our knowledge, the lowest published threshold to date for any Yb-doped laser. The effect of Yb^{3+} concentration on laser threshold is experimentally quantified.

© 2007 Optical Society of America

OCIS codes: 140.3070, 140.5680, 140.3560.

Rare-earth ions (e.g., Er^{3+} , Nd^{3+} , Yb^{3+} , Ho^{3+}) are popular dopants for solid-state lasers due to their high efficiencies, long upper-level lifetimes, ability to generate short pulses, and straightforward incorporation into host materials including glasses and crystals [1]. In addition, the rare-earth aggregate emission spectrum spans many key wavelengths from 0.3 to 3 μm that are important for imaging, sensing, medical treatment, and communications. While rare-earth lasers have been built in large form factors for high-power laser cutting and defense applications, they can also be designed to be small, low power, and ultrasensitive to the environment. The laser resonator finesse, defined as the free spectral range (FSR) divided by the resonance linewidth, quantifies the loss and hence energy storage efficiency of a resonator. For a given cavity, higher finesse results in lower threshold for lasing. Lacovara *et al.* measured a 71 mW threshold for a $\text{Yb}^{3+}:\text{YAG}$ microchip laser with a cavity finesse of 57 [2]. Asseh *et al.* demonstrated 230 μW threshold for a $\text{Yb}^{3+}:\text{SiO}_2$ fiber laser with a finesse of 630 [3]. Recently, the ultrahigh- Q ($>10^8$) toroid whispering-gallery resonator was invented [4]. The extremely low loss of this device enabled significant reduction of the threshold for an Er-doped silica solgel laser [5]. The Yb silica toroid microcavity laser reported in this Letter has an on-resonance finesse greater than 10,000.

The Yb-doped silica gain medium of this microlaser is fabricated on a silicon chip according to the solgel chemical synthesis method. The solgel technique for making thin films is attractive because it is low cost, fast, and extremely flexible [6]. Indeed, solgel techniques have been used to make optical couplers, $\text{Er}^{3+}-\text{Yb}^{3+}$ -doped waveguide amplifiers, and even silica nanotubes [7–9]. A $\text{Yb}^{3+},\text{Al}^{3+}:\text{SiO}_2$ solgel fiber laser achieved a threshold of 80 mW launched power [10]. We present a fiber-coupled Yb-doped silica solgel microtoroid laser with 1.8 μW threshold, which is believed to be the lowest threshold to date for any Yb laser.

Fabrication of the laser microcavity begins with solgel synthesis of the Yb-doped silica thin film. First, tetraethoxysilane (TEOS) is hydrolyzed with a molar ratio of water to TEOS between 1:1 and 2:1. Isopropanol is the cosolvent and hydrochloric acid the catalyst. After the alkoxide groups in TEOS are replaced with hydroxyl groups, the remaining hydrogen atoms are removed through a condensation reaction. Finally, Yb nitrate is introduced to produce the desired Yb^{3+} concentration in the silica thin film. The entire mixture is stirred on a hot plate at 70°C for 3 h to produce the solgel liquid. Next, the Yb-doped silica solgel is deposited in three layers onto a silicon substrate by spin coating. Immediately after each layer deposition, the thin film is annealed at 1,000°C in normal atmosphere for 3 h to remove the solvent, undesired organics, and hydroxyl groups in the solgel network [11,12]. Afterwards, the glass film is patterned by standard lithography and isolated silica disks are defined on the silicon substrate using a buffered oxide wet etch. The disks are then optically isolated from the underlying silicon using XeF_2 to selectively etch silicon, leaving $\text{Yb}^{3+}:\text{SiO}_2$ disks supported by silicon pillars. In the final step, a CO_2 laser ($\lambda=10.6 \mu\text{m}$) symmetrically reflows the silica microdisk to form a smooth microtoroid with a 40 μm principal diameter. Surface tension during melting defines the toroid shape and increases the cavity quality factor by significantly reducing surface roughness.

A single submicrometer diameter fiber taper, which is phase matched to the microcavity's whispering-gallery spatial mode, couples light into and out of the microtoroid at the equatorial plane as shown in Fig. 1 [13,14]. The coupling parameter, which determines the cavity loading and consequently the laser performance, is precisely adjusted by moving the silica cavity with respect to the fiber taper using a three-axis nanopositioning system. A tunable, single-frequency, narrow linewidth ($<300 \text{ kHz}$) semiconductor diode laser provides pump light in the 970 nm absorption

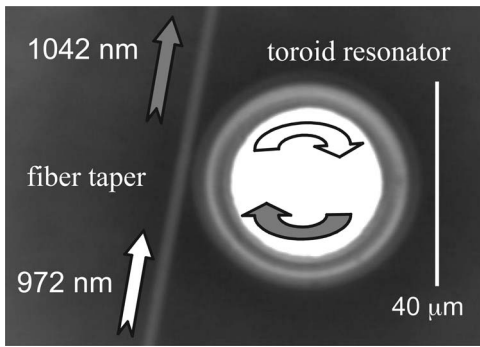


Fig. 1. Top-view photograph of testing setup showing evanescent coupling of fiber taper to $\text{Yb}^{3+}:\text{SiO}_2$ microcavity.

band of Yb. At the fiber output, $\text{Yb}^{3+}:\text{SiO}_2$ laser emission at 1042 nm and unabsorbed pump light at 972 nm are separated by a fiber-coupled WDM filter with 45 dB isolation. The coupling and laser output are monitored with an optical detector, powermeter, and spectrum analyzer (0.07 nm resolution). The intrinsic microcavity quality factor is calculated by measuring the resonance linewidth in the under-coupled regime. At the pump wavelength of 972 nm, the Q is 1×10^6 due to resonant absorption by the Yb^{3+} ions. The cavity Q at 1550 nm, well removed from the Yb absorption band, is 25×10^6 and reflects the low scattering loss of the cavity.

Since the average pump photon makes $\sim 1,000$ round trips in the cavity, this Yb-doped glass laser achieves efficient pump absorption even though the Yb concentration is just 0.01 at. %. High pump absorption, short cavity length, and low doping concentration are necessary for low lasing threshold [15]. The doping concentration must be high enough to provide sufficient gain to overcome material and cavity losses. As such, no lasing was observed for Yb concentrations as low as $1\text{--}2 \times 10^{18} \text{ cm}^{-3}$ given the available pump power. But for concentrations greater than at least $4 \times 10^{18} \text{ cm}^{-3}$, the pump threshold was measured to increase with concentration as shown in Fig. 2. The additional pump power is needed to compensate for the loss from unpumped Yb^{3+} ions be-

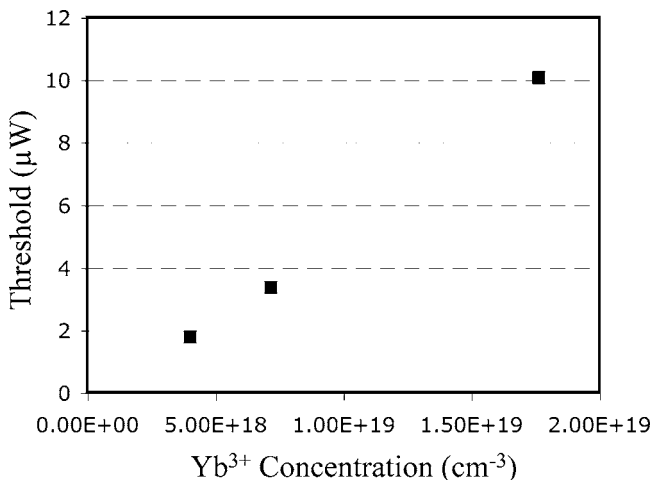


Fig. 2. Measured laser threshold (absorbed power) as a function of Yb^{3+} concentration for Yb-doped silica microcavity.

cause the ground state of Yb is well populated at room temperature.

We achieved 1.8 μW threshold of absorbed power for a 40 μm diameter silica microtoroid laser with $4 \times 10^{18} \text{ cm}^{-3}$ Yb^{3+} concentration. To the best of our knowledge, this is the lowest published threshold to date for any Yb-doped laser. The laser output power depends linearly on the absorbed pump power (above threshold) as shown in Fig. 3. The coupler, filter, and taper losses are accounted for in these results. Microtoroids support both clockwise and counterclockwise modes that are coupled by surface scattering [16]. But we measure the single-end laser power from only the clockwise mode, discarding approximately half of the laser output power. While the laser slope efficiency with respect to absorbed power for the lowest threshold laser is 3%, we measured slope efficiency as high as 18%, as shown in Fig. 3. The highest output power is 12 μW .

We observed continuous wave (cw) multimode lasing over a 40 nm span for certain taper to cavity couplings conditions, due to the broad emission bandwidth of Yb. But, with proper alignment, single-frequency cw laser output is attainable (see the laser spectrum shown in Fig. 4). The microtoroid laser cavity FSR is 6 nm. It is also possible to excite modes that experience pulsations in the laser output power similar to those found in an $\text{Er}^{3+}:\text{SiO}_2$ microtoroid laser [5]. Pulsing is most easily observed for higher doping concentration (typically $2 \times 10^{19} \text{ cm}^{-3}$), and pulsing with 1 MHz repetition rate and 200 ns duration was measured. The origin and behavior of pulsations in Yb-doped silica microlasers is believed to be associated with saturable absorption of the Yb ions [17].

In conclusion, we have demonstrated a single-frequency on-chip Yb-doped silica laser fabricated by the sol-gel process. The pump threshold is as low as 1.8 μW , which is more than 100 times less than the lowest published threshold to date for a Yb-doped laser [3]. The slope efficiency is as high as 18%. This

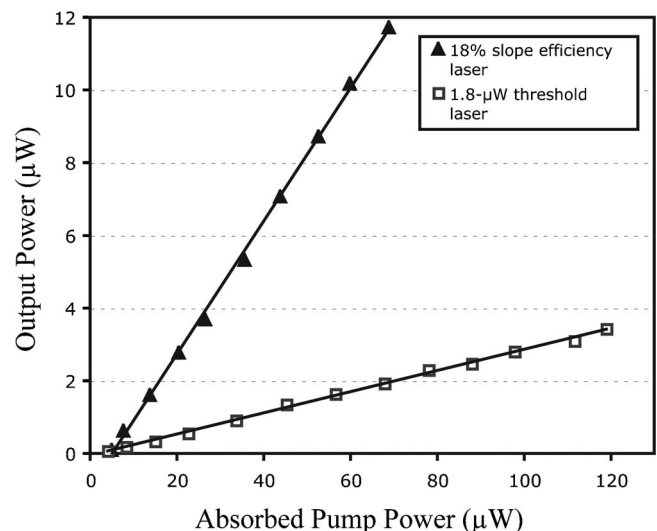


Fig. 3. Measured laser output power as a function of absorbed pump power for two 40 μm diameter $\text{Yb}^{3+}:\text{SiO}_2$ microtoroid lasers.

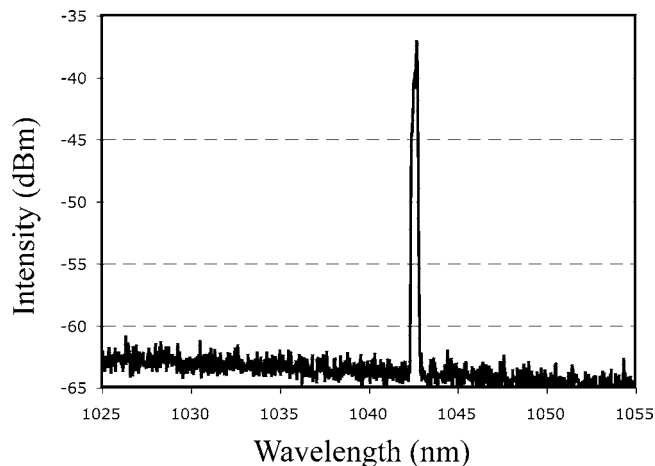


Fig. 4. Measured laser output spectra of single-frequency $\text{Yb}^{3+}:\text{SiO}_2$ microtoroid laser.

$\text{Yb}^{3+}:\text{SiO}_2$ laser will operate more efficiently in a water environment compared with a $1.55\ \mu\text{m}$ laser, since the absorption coefficient of water is significantly less at $1.0\ \mu\text{m}$ compared with $1.55\ \mu\text{m}$ (0.16 and $12\ \text{cm}^{-1}$, respectively) [18]. As such, it could function as the laser for an active chemical or biological sensor using surface functionalization protocols readily available for silica. Also, the flexible sol-gel process and compatibility of the simple electronic structure of Yb with other rare-earth ions can be used in the future for dual-doped lasers such as $\text{Er}^{3+}, \text{Yb}^{3+}:\text{SiO}_2$; a subnanosecond Q -switched $\text{Cr}^{4+}, \text{Yb}^{3+}:\text{SiO}_2$ laser [19]; or upconversion lasers [20]. Applications for this low threshold and small footprint laser may be found in dense on-chip optical communications, active sensors, and rare-earth visible lasers.

This work was financially supported by MURI grant FA9550-04-1-0434 and the Defense Advanced Research Projects Agency (DARPA) Center for Optofluidic Integration.

References

1. E. P. Ostby, J. M. Fukumoto, R. D. Stultz, S. Matthews, and D. Filgas, *Proc. SPIE* **5707**, 72 (2005).
2. P. Lacovara, H. K. Choi, C. A. Wang, R. L. Aggarwal, and T. Y. Fan, *Opt. Lett.* **16**, 1089 (1991).
3. A. Asseh, H. Storoy, J. T. Kringlebotn, W. Margulis, B. Sahlgren, S. Sandgren, R. Stubbe, and G. Edwall, *Electron. Lett.* **31**, 969 (1995).
4. D. K. Armani, T. J. Kippenberg, S. M. Spillane, and K. J. Vahala, *Nature* **421**, 925 (2003).
5. L. Yang, T. Carmon, B. Min, S. M. Spillane, and K. J. Vahala, *Appl. Phys. Lett.* **86**, 091114 (2005).
6. L. L. Hench, and J. K. West, *Chem. Rev. (Washington, D.C.)* **90**, 33 (1990).
7. C. Y. Li, J. Chisham, M. Andrews, S. I. Najafi, J. D. Mackenzie, and N. Peyghambarian, *Electron. Lett.* **31**, 271 (1995).
8. J. E. Meegan, A. Aggeli, N. Boden, R. Brydson, A. P. Brown, L. Carrick, A. R. Brough, A. Hussain, and R. J. Ansell, *Adv. Funct. Mater.* **14**, 31 (2004).
9. X. Orignac, D. Barbier, X. M. Du, R. M. Almeida, O. McCarthy, and E. Yeatman, *Opt. Mater.* **12**, 1 (1999).
10. U. Pedrazza, V. Romano, and W. Luthy, *Opt. Mater.* **29**, 905 (2007).
11. A. S. Holmes, R. R. A. Syms, M. Li, and M. Green, *Appl. Opt.* **32**, 4916 (1993).
12. G. Brusatin, M. Guglielmi, P. Innocenzi, A. Martucci, C. Battaglin, S. Pelli, and G. Righini, *J. Non-Cryst. Solids* **220**, 202 (1997).
13. S. M. Spillane, T. J. Kippenberg, O. J. Painter, and K. J. Vahala, *Phys. Rev. Lett.* **91**, 043902 (2003).
14. M. Cai, O. Painter, and K. J. Vahala, *Phys. Rev. Lett.* **85**, 74 (2000).
15. B. K. Min, T. J. Kippenberg, L. Yang, K. J. Vahala, J. Kalkman, and A. Polman, *Phys. Rev. A* **70**, 033803 (2004).
16. T. J. Kippenberg, S. M. Spillane, and K. J. Vahala, *Opt. Lett.* **27**, 1669 (2002).
17. L. Yang and K. J. Vahala, *Opt. Lett.* **28**, 592 (2003).
18. G. M. Hale and M. R. Querry, *Appl. Opt.* **12**, 555 (1973).
19. Y. Zhou, Q. Thai, Y. C. Chen, and S. H. Zhou, *Opt. Commun.* **219**, 365 (2003).
20. M. Zeller, H. G. Limberger, and T. Lasser, *IEEE Photon. Technol. Lett.* **15**, 194 (2003).